2023 IEEE/ASME International Conference on Advanced Intelligent Mechatronics (AIM)
June 28-30, 2023. Seattle, Washington, USA

Validation of Feedforward Disturbance Cancellation for the PSS3 HDD Benchmark Problem for Dual Stage Actuators

Yuma Tanaka, Jun Ishikawa, *Member, IEEE*

Abstract— **This article proposes a method of feed-forward cancellation of disturbance effects and reports on the results of verifying its performance using the controller included with the dual-stage actuator and a newly designed controller for the magnetic disk device benchmark problem proposed by the Investigating R&D Committee on Basis of Collaborative Technologies for Precision Servo Systems (PSS3). As a result of the verification, the controller with the proposed method was able to reduce the displacement of the PZT actuator, confirming the effectiveness of the proposed method.**

I. INTRODUCTION

In recent years, solid state drives (SSDs) have made a remarkable comeback as a medium for storing data, competing with magnetic disk drives (HDDs) and separating the two. Compared to SSDs, HDDs have the advantages of low unit cost per data volume and the ability to store large amounts of data [1]. On the other hand, SSDs are characterized by their high write speed and shock resistance [2]. Because of these advantages, HDDs are used as the primary storage device in large data centers because of their low cost per data volume and large data storage capacity [3]. However, because HDDs read and write data by physically moving the platter and head, they are susceptible to external and internal vibrations [4]. In particular, when used in data centers, vibrations transmitted from surrounding HDDs and air-cooling fans inside file servers are one of the causes of degraded positioning accuracy [5]-[7].

Based on this background, the Investigating R&D Committee on Basis of Collaborative Technologies for Precision Servo Systems (PSS3) proposed a benchmark problem for improving control performance and objective evaluation [8]. The benchmark problem targets a dual-stage HDDs, which has become mainstream in recent years, and uses a configuration with a voice coil motor (VCM) in the first stage and a piezoelectric (PZT) actuator in the second stage.

One method for improving the positioning performance of two-stage HDDs is to treat the control target, which is originally a Multi Input Single Output (MISO) system, as a Single Input Single Output (SISO) system by performing decoupling [9]. Other methods include those that apply acceleration feedforward control [10]. In a previous study [11] in which the authors added acceleration feedforward control to the benchmark problem and verified its effectiveness, the displacement of the PZT actuator was much larger than the allowable range of 50 nm. We believe that this is because the benchmark problem did not assume the application of acceleration feedforward control, which caused a large displacement of the PZT actuator.

Therefore, in this paper, the controller is improved to prevent large displacement of the PZT actuator even if acceleration feed-forward control is applied. Specifically, this paper proposes that the signal input to the PZT actuator be input to the VCM in order to suppress the displacement of the PZT actuator. In addition, the acceleration feed-forward control is applied to the controller that has been improved by trial and error to improve the positioning performance.

II. BENCHMARK PROBLEM

A. Overview of Benchmark Problems

The control system under study is based on a benchmark problem, and its configuration is shown in Fig. 1.

Where $P_{cp}(s)$ is the mechanical system characteristics of the PZT actuator as a continuous time function system, $P_{cv}(s)$ is the VCM mechanical system characteristics as a continuous time function system, $F_{mp}(z)$ is a multi-rate filter for PZT actuators, $F_{mv}(z)$ is a multi-rate filter for VCM, $C_{dp}(z)$ is the discrete-time controller for PZT actuators, $C_{dv}(z)$ is the discrete-time controller for VCM. H_m is the multirate hold, $I_p(z)$ is the interpolator, S_1 and S_2 are samplers. where the sampling time T_s of sampler S_1 is $19.841\,\mu s$ and The sampling time $T_s/2$ of sampler S_2 is $9.920\,\mu s$, the number of multirates used for the multirate hold H_m and interpolator $I_p(z)$ is 2.

For the signals, r is the reference value, e is the error, y_{cp} is the displacement of the PZT actuator in continuous time, u_{pzt} is the input value of $P_{cp}(s)$, u_{vcm} is the input value of $P_{cv}(s)$, y_c is the magnetic head position in continuous time, y_{d1} is the magnetic head position sampled at T_s, y_{d2} is the magnetic head position virtually sampled at $T_s/2$, which are used to calculate the transfer function. For disturbances, d_{RRO}, d_f, and d_p represent the effect of RRO, vibration transmitted from surrounding hard disks, and vibration caused by air cooling fans in the file server, respectively, converted to the

Y. Tanaka and J. Ishikawa are with the Department of Robotics and Mechatronics, Tokyo Denki University, 5 Senju Asahi-cho, Adachi-ku, Tokyo 120-8551, Japan (Phone: +81-3-5284-5607; fax: +81-3-5284-5698, email: ishikawa@mail.dendai.ac.jp).

position dimension. Since the effect of vibration caused by air cooling fans is converted to the position dimension, the effect on the position error signal is equivalent, but the method (dimension) of application may need to be modified when considering compensation. The control target and multirate filter given as a benchmark problem are shown in Fig. 2 and Fig. 3.The transfer functions to be controlled are curve-fitted from actual measurements, and the three disturbance signals are periodic disturbances with a d_{RRO} of 120 Hz, and the main frequencies for d_f and d_p are around 300 Hz and around 4000~6000 Hz, respectively. For reasons of space, the details are omitted; refer to references [8] and [12].

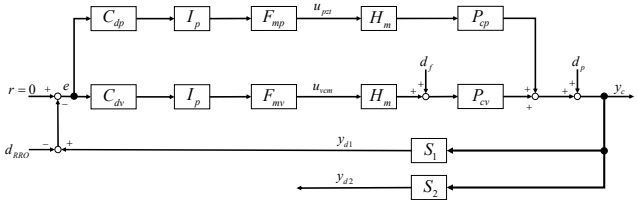

Figure. 1. Block diagram of the herd disk drive head positioning control system in the benchmark problem

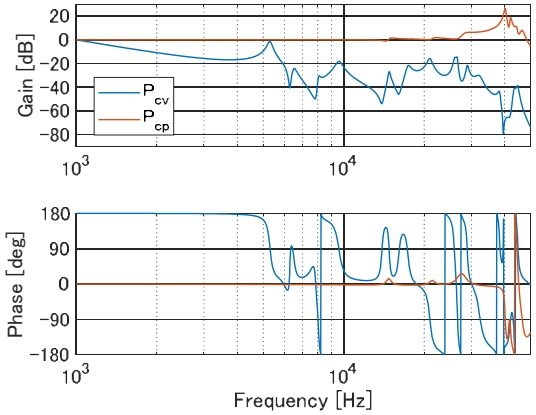

Figure. 2. Frequency response of VCM and PZT actuator mechanical system characteristics in continuous time: $P_{cv}(s)$ (blue line), $P_{cp}(s)$ (red line) in Fig.1.

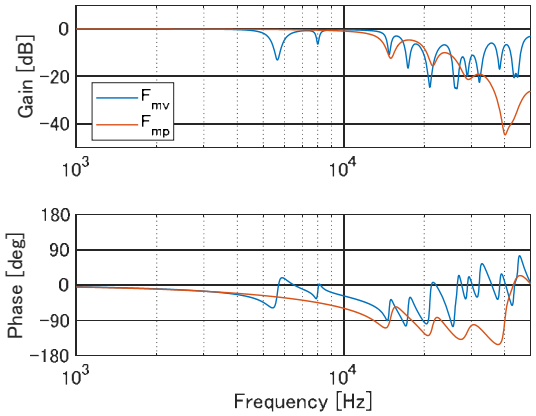

Figure. 3. Frequency response of multi-rate filter for VCM and PZT actuator: $F_{mv}(z)$ (blue line), $F_{mp}(z)$ (red line) in Fig.1.

B. Controllers attached to the benchmark problem

Fig. 4 shows the controller attached to the benchmark problem. The simulated 3σ value is 6.9443 nm, and the y_c displacement and amplitude spectra are shown in Fig. 5. The right panel of Fig. 5 shows that the amplitudes are large around 250 Hz and 2500-6700 Hz.

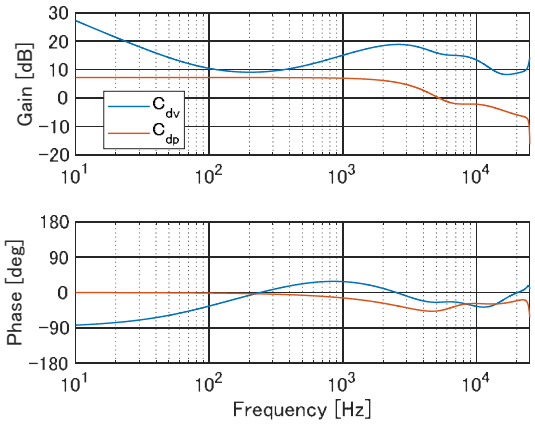

Figure. 4. Frequency response of discrete-time controllers for VCM and PZT actuator: $C_{dp}(z)$ (blue line), $C_{dv}(z)$ (red line) in Fig. 1.

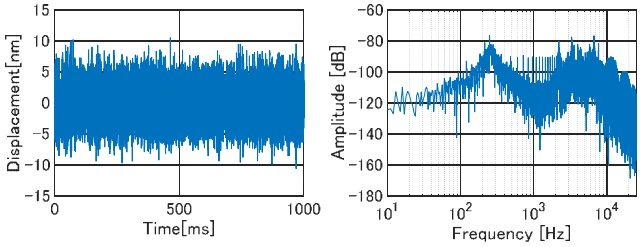

Figure. 5. The displacement and amplitude spectrum of y_c

III. DESIGN OF HEAD POSITIONING CONTROL SYSTEM

A. Design guidelines for this project

In designing the new controller, the following three guidelines were established.

- Design with the hypothesis that since the PZT actuator can move to a high bandwidth, the value input to the PZT actuator can be added to the VCM controller to reduce the displacement of the PZT actuator.
- Design a stable controller for each of the VCM and PZT actuators (The VCM controller that is attached to the benchmark problem could not stabilize the controlled plant when it is used alone).
- With the supplied controller, adding acceleration feedforward control would greatly exceed 50 nm, the limit of the motion range of the PZT actuator, so a controller that does not exceed 50 nm should be designed.

B. Designed control system and controller

From the design guideline shown in the first item of Section III-A, the block diagram shown in Fig. 1 was modified as shown in Fig. 6. Next, based on the design guideline shown in the second item of Section III-A, stable controllers were designed for the VCM and PZT actuators, respectively. where $C_{dv}(z)$ is a PID controller and $C_{dp}(z)$ consists of a phase lead compensator and an integrator. The PID controller is given as follows:

$$C_{dv}(z) = K_p + K_i \cdot T_s \frac{1}{z-1} + K_d \frac{N}{1 + N \cdot T_s \dfrac{1}{z-1}} \qquad (1)$$

The phase lead compensator and integrator are given as follows:

$$C_{dp}(s) = \frac{Ts+1}{\alpha Ts+1} \cdot \frac{1}{s} \quad (\alpha < 1) \qquad (2)$$

Where, the parameters for designing equations (1) and (2) are as shown in Table 1. The VCM controller was designed first, followed by the PZT actuator controller. The target bandwidth on the VCM side was set at 700 - 800 Hz, and then the PZT actuator controller was designed to improve positioning performance. In addition, focusing on the frequency bandwidth of the disturbance applied to the HDDs, the controller was designed to lower the sensitivity function around 4000 Hz. Since the design is currently being conducted on a trial-and-error basis, the theoretical design method is an issue to be addressed in the future. The frequency responses of the designed controller are shown in Fig. 7 and Fig. 8.

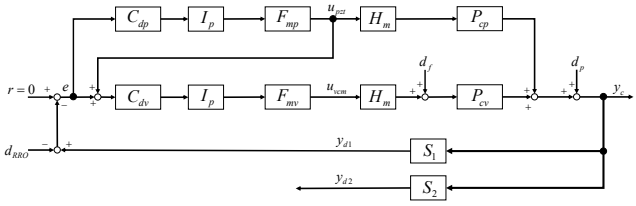

Figure. 6. Block diagram with modifications to Fig. 1.

Table 1. Controller Parameters

variable name	value	unit
K_p	0.5	$1/s^2$
K_i	100	$1/(\mathrm{m} \cdot s^2)$
K_d	15×10^{-5}	1/s
N	10000	$1/s^2$
T	1.8967×10^{-4}	s
α	0.7041	-

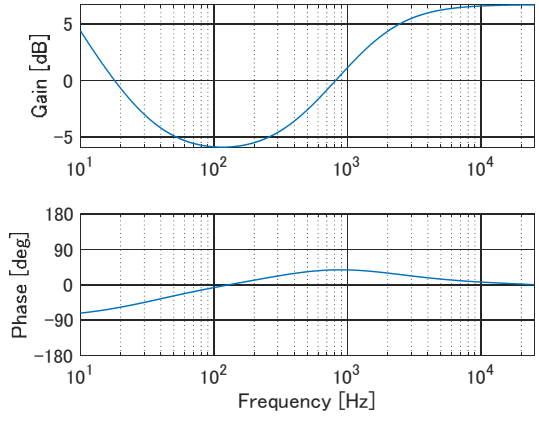

Figure. 7. Frequency response of discrete-time controllers for VCM

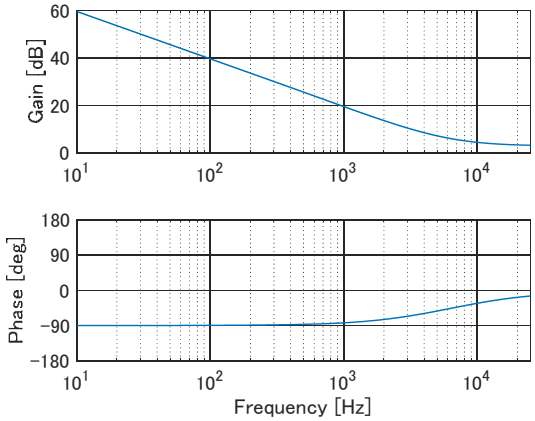

Figure. 8. Frequency response of discrete-time controllers for PZT actuator

C. *Comparison with the proposed controller in the benchmark problem*

In this section, The controller proposed in section III-B and the controller included with the benchmark problem are compared against their respective performance. The comparison will be made using the sensitivity functions from d_f to y_c and from d_p to y_c, the 3σ value of y_c converted to a percentage of the track pitch. Fig. 9 shows the frequency response from d_f to y_c, Fig. 10 shows the frequency response from d_p to y_c, and Table 2 shows the 3σ value of y_c as a percentage of the track pitch (track pitch is 52.697 nm). Table 2 shows that the performance is better with the proposed controller. Fig. 9 shows that the disturbance effect does not have much influence on the displacement *i.e.*, the position error signal, since it does not exceed 0 dB for both controllers. Fig. 10 shows that the controller attached to the benchmark problem increased to about 5 dB around 4000 Hz, but the proposed controller was below 0 dB around 4000 Hz. This was designed with the main frequency band of disturbance (described in section III-B) around 4000 Hz in consideration of lowering the frequency band.

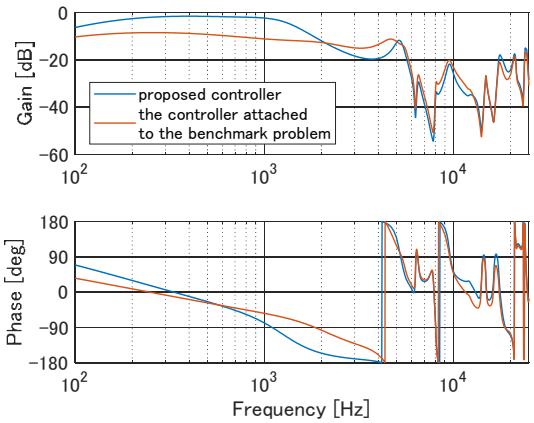

Figure. 9. Frequency response from d_f to y_c

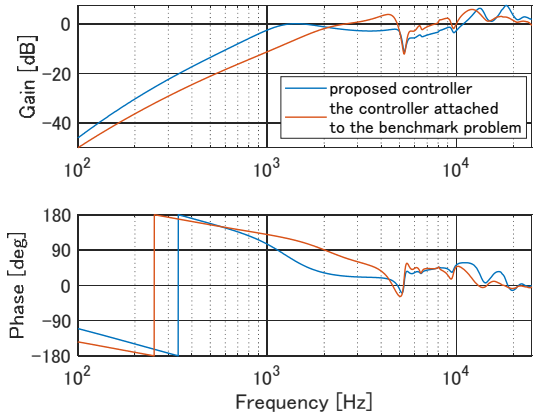

Figure. 10. Frequency response from d_p to y_c

Table.2 3σ value of y_c converted to a percentage of track pitch.

proposed controller	the controllers attached to the benchmark problem
10.6894%	13.1778%

IV. IMPROVED POSITIONING PERFORMANCE THROUGH ACCELERATION FEEDFORWARD CONTROL

In this section, assuming that the vibration d_f transmitted from the surrounding HDDs can be obtained with a sampling time T_s by attaching an acceleration sensor to the disk enclosure, a method to cancel the effect of the vibration will be implemented and evaluated. The transfer function from u_{pzt} to y_{d2} is given by

$$y_{d2} = G_1(z)u_{pzt} \tag{3}$$

The transfer function from d_f to y_{d2} is given by

$$y_{d2} = G_2(z)d_f \tag{4}$$

Then u_{pzt}, which cancels the effect of d_f can be calculated as follows:

$$u_{pzt} = -G_1^{-1}G_2 d_f \tag{5}$$

Adding u_{pzt} as an input can reduce the effect of noise. If the controller attached to the benchmark is used as is, $G_1(z)^{-1}G_2(z)$ has an integral characteristic, as shown in Fig. 8 below, and large displacements occur in the PZT actuator for low-frequency disturbances. Therefore, the low-frequency component of the disturbance d_f is simply blocked by a high-pass filter (HPF) before the disturbance is suppressed. The disturbance compensation filter is designed and created using Simulink provided by MathWorks by constructing a block diagram as shown in Fig. 1 and Fig. 6.

A. *Disturbance compensation filter design for the proposed controller*

The dlinmod function is used to obtain a linear model (state-space representation) between specified inputs and outputs on a Simulink block around the equilibrium point that Simulink has, and the n4sid function is used to obtain a state-space representation of a specified order from the frequency response.

Step1. The state space representation corresponding to the transfer function $G_1(z)$ in (3) is derived by the function dlinmod. The sampling time is $T_s/2$, and y_{d2} is used as the output (the sampler is S_2).

Step2. As in Step 1, the model of the transfer function in (4) is derived in the state space representation.

Step3. Using these state-space representations, the state-space representation corresponding to (5) is obtained. Since the derived model has a high order (173rd order in this example), its frequency response is first calculated. The frequency range of interest for the frequency response is specified and the filter is lowered in dimension using the n4sid function, which can fit the frequency response of a model of any order of the state-space representation to the frequency response in that range (in this case, the 173rd order model is lowered to 12th order. As a result of trial and error to keep the order as small as possible within the range where resonance and other parameters within the assumed control band can be reproduced, the order was determined to be 12th order.). Fig. 11 shows the frequency response $G_1(z)^{-1}G_2(z)$ (173rd order) of the transfer function obtained using (5) and the frequency response of the transfer function approximated by the 12th order. The blue line in Fig. 11 is the frequency response of the transfer function obtained using (5), and the red dashed line is the approximation of the transfer function using the 12th order. The red dashed line shows that it can be approximated from 100 Hz to about 10 kHz.

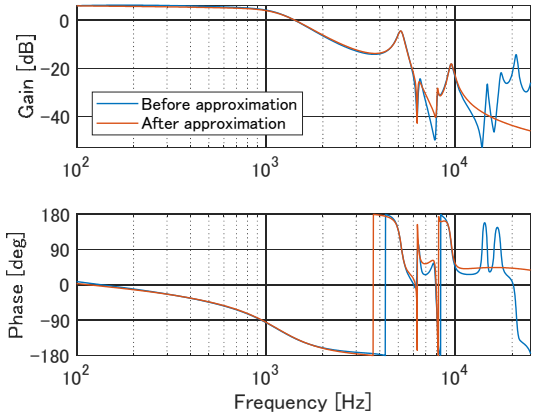

Figure. 11 Disturbance compensation filter for the proposed controller

B. *Disturbance compensation filter design for controllers attached to the benchmark problem*

In addition to the steps explained in section IV-A, applying an HPF to the lower-dimensionalized filter to block the low frequency component of the disturbance is used to reduce the displacement of the PZT actuator. As for the cutoff frequency of the HFP, it was set at 100 Hz. This was chosen because 100 Hz was the most effective in a study [7] that investigated the

performance of acceleration feedforward when the cutoff frequency was varied. Thus, one advantage of Simulink-based development is that one can intuitively consider where in the control system to implement a filter with what characteristics and can easily evaluate controller performance through trial and error (e.g., by changing various input points). This design procedure is as follows.

Step1. Design the filter on the PZT actuator side in the same manner as in Step 1 through Step 3 of Section IV-A. Fig. 12 shows the frequency response $G_1(z)^{-1}G_2(z)$ (173rd order) of the transfer function derived using (5) as well as the frequency response of the transfer function approximated by 12th order. The blue line in Fig. 12 is the frequency response of the transfer function derived using (5), and the red dashed line is the approximation of the transfer function with 12th order. The red dashed line shows that it can be approximated from 100 Hz to about 10 kHz.

Step.2 The lower dimensionalized filter is further subjected to an HPF with a cutoff frequency of 100 Hz to block the low-frequency component of the disturbance and suppress the displacement of the PZT actuator.

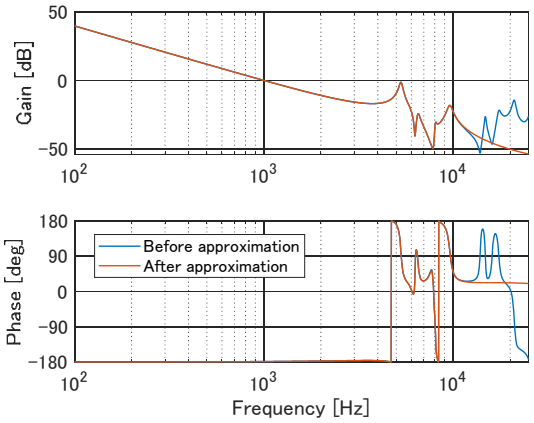

Figure. 12 Disturbance compensation filters for controllers attached to the benchmark problem

C. *Disturbance compensation filter results for the proposed controller and the controller included with the benchmark problem*

The block diagram with the disturbance compensation filter designed in Sections IV-A and IV-B is shown in Fig. 13. The blue boxes in Fig. 13 show the acceleration feedforward control and HPF blocks added this time. The control system in Fig. 13 was used for the simulation, and the 3σ values of y_c converted to a percentage of the track pitch are shown in Table 3 and the amplitude spectrum of y_c is shown in Fig. 14. The displacements of the VCM and PZT actuator for the proposed controller and the controller attached to the benchmark problem are shown in Fig. 15 and Fig. 16. Table 3 shows that the performance of both controllers improved after the addition of acceleration feedforward control. Furthermore, Fig. 14 shows that after applying acceleration feedforward control to both controllers, the effect of the main frequency band of disturbance d_f, around 300 Hz, was reduced. Fig. 15 shows that the displacement of the PZT actuator of the proposed controller was suppressed to within 50 nm. In contrast, the displacement of the PZT actuator of the controller attached to the benchmark problem is much larger than 50 nm, as shown in Fig. 15. This discussion will examine the cause of the difference in the displacement of the PZT actuator between the two controllers. Fig. 16 and Fig. 17 show the characteristics from d_f to u_{pzt}, respectively. In the proposed controller shown in Fig. 16, the effect of the disturbance d_f on the input u_{pzt} of the PZT actuator is about 6 dB at maximum and does not cause a large displacement. On the other hand, Fig. 17 shows that for the controller attached to the benchmark problem, the disturbance d_f exceeds 0 dB at frequencies below 1 kHz, and the lower the frequency, the greater the amplification of the disturbance d_f. This suggests that the controller attached to the benchmark problem amplified the displacement of the PZT actuator. From the above, it is confirmed that the proposed controller can suppress the displacement of the PZT actuator. In the benchmark problem [12], a total of 9 cases of control targets were prepared assuming temperature dependence and characteristic variation due to PZT actuator gain variation. As a result of the evaluation for these nine cases, the proposed controller falls within the range of 10.3684% to 11.5424% in terms of the 3σ value of y_c as a percentage of the track pitch.

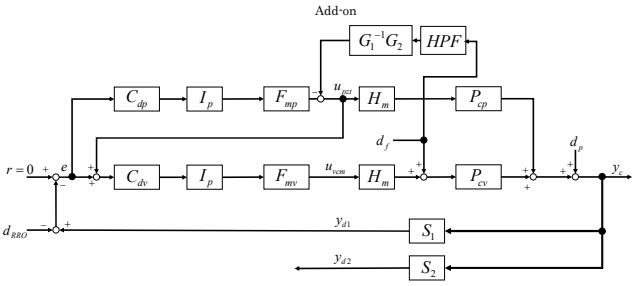

Figure. 13 Block diagram of control system with additional filters in Fig. 11 and Fig. 12

Table.3 3σ values of y_c converted to a percentage of track pitch: before (left side) and after (right side) application of acceleration feedforward control

Proposed Controller		**Controllers attached to the benchmark problem**	
Before application	**after application**	**Before application**	**after application**
10.6894%	10.6672%	13.1778%	12.7565%

V. Conclusion

In this study, acceleration feedforward control was added to the proposed controller in comparison with the controller included with the benchmark problem. The results of the study confirmed that both controllers were able to reduce the influence of disturbances, and the proposed controller was

able to control without causing large displacements.

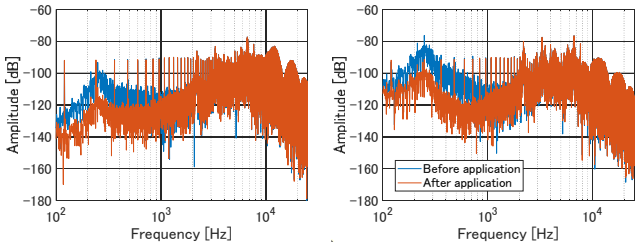

(a) proposed controller (b) the controller attached to the benchmark problem

Figure. 14 Amplitude spectrum of y_c

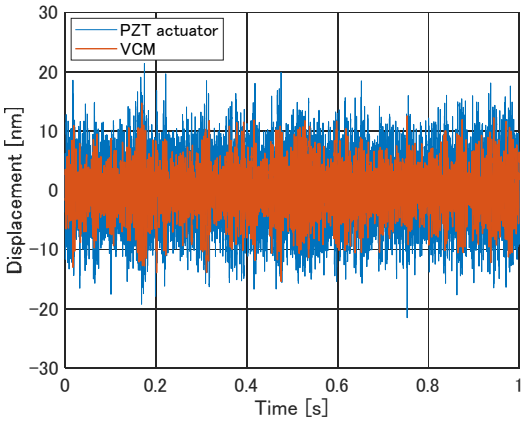

Figure. 15 Displacement of VCM and PZT actuator with the proposed controller

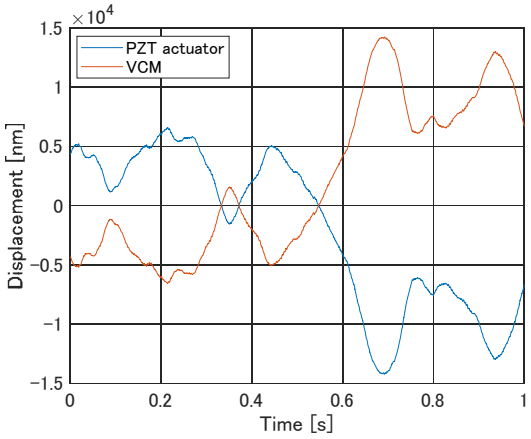

Figure. 16 Displacement of VCM and PZT actuator with the controller attached to the benchmark problem

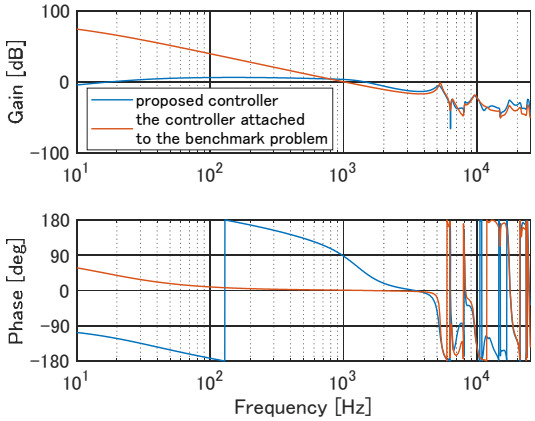

Figure. 17 Transfer function from d_f to u_{pzt} :

REFERENCES

[1] Seongjin Lee, Seokhui Cho, Haesung Kim and Youjip Won, "Performance analysis of SSD/HDD hybrid storage manager," *The 16th North-East Asia Symposium on Nano, Information Technology and Reliability*, Macao, China, 2011, pp. 136-139, doi: 10.1109/NASNIT.2011.6111135.

[2] P. Saxena and P. Kumar, "Performance evaluation of HDD and SSD on 10GigE, IPoIB & RDMA-IB with Hadoop Cluster Performance Benchmarking System," *2014 5th International Conference - Confluence The Next Generation Information Technology Summit (Confluence)*, Noida, India, 2014, pp. 30-35, doi: 10.1109/CONFLUENCE.2014.6949047.

[3] T. Iwamoto, " Large-Capacity HDD Technologies for Data Society with Capability to Handle Huge Volumes of information" TOSHIBA REVIEW, Vol.76, No.6, 2021.

[4] T.Yamaguchi, M Hirata, H.Fujimoto, "Nanoscale Servo Technology - High Speed and High Precision Positioning Technology-" TDU Press,2007, (in Japanese).

[5] T. Shimizu, O. Tatebe and T. Kudoh, "The effects of cooling fanvibration on hard disk drives." *Transaction of Information ProcessingSociety of Japan2004*,45(6):23 – 34 (in Japanese).

[6] T. Eguchi, K. Ichikawa, S. Takada and M. Takada, "High Frequency Dynamics of a HDD in a Storage Server: Airborne Vibration Transmission and PES Simulations," *2018 Asia-Pacific Magnetic Recording Conference (APMRC)*, Shanghai, China, 2018, pp. 1-1, doi: 10.1109/APMRC.2018.8601030.

[7] Xianguang Tan, Guofeng Chen, Jiajun Zhang, Chao Liu, Nishi Ahuja and Jun Zhang, "An advanced rack server system design For Rotational Vibration (RV) performance," *2016 15th IEEE Intersociety Conference on Thermal and Thermomechanical Phenomena in Electronic Systems (ITherm)*, Las Vegas, NV, 2016, pp. 1320-1325, doi: 10.1109/ITHERM.2016.7517701.

[8] T. Atsumi and S. Yabui, "Quadruple-Stage Actuator System for Magnetic-Head Positioning System in Hard Disk Drives," in *IEEE Transactions on Industrial Electronics*, vol. 67, no. 11, pp. 9184-9194, Nov. 2020, doi: 10.1109/TIE.2019.2955432.

[9] O. Bagherieh and R. Horowitz, "Mixed H2/H∞ Data-Driven Control Design for Hard Disk Drives," *2018 Asia-Pacific Magnetic Recording Conference (APMRC)*, Shanghai, China, 2018, pp. 1-3, doi: 10.1109/APMRC.2018.8601117.

[10] C. Du, S. S. Ge, F. L. Lewis and J. Zhang, "External vibration compensation via loop shaping and H∞ feedforward control design for hard disk drives in mobile applications," *2007 IEEE 22nd International Symposium on Intelligent Control*, Singapore, 2007, pp. 277-282, doi: 10.1109/ISIC.2007.4450898.

[11] Y. Tanaka, J Ishikawa, "Validation of Feedforward Disturbance Cancellation for the PSS3 HDD Benchmark Problem for Dual Stage Actuators", *Mechatronics Control Research Group*,2022(in Japanese).

[12] https://jp.mathworks.com/matlabcentral/fileexchange/111515-magnetic-head-positioning-control-system-in-hdds